ЖЭТФ, 2012, том 142, вып. 3 (9), стр. 480–486

THE RATIO OF THE CHARM STRUCTURE FUNCTIONS F_k^c $(k = 2, L)$ AT LOW x IN DEEP INELASTIC SCATTERING WITH RESPECT TO THE EXPANSION METHOD

G. R. Boroun[*], *B. Rezaei*[**]

Physics Department, Razi University
67149, Kermanshah, Iran

Received February 2, 2012

We study the expansion method for the gluon distribution function at low x values and calculate the charm structure functions in the LO and NLO analysis. Our results provide a compact formula for the ratio $R^c = F_L^c/F_2^c$, which is approximately independent of x and the details of the parton distribution function at low x values. This ratio could be a good probe of the charm structure function F_2^c in the proton deduced from the reduced charm cross sections at DESY HERA. These results show that the charm structure functions obtained are in agreement with HERA experimental data and other theoretical models.

1. INTRODUCTION

The low-x regime of the quantum chromodynamics (QCD) has been intensely investigated in recent years for consideration of the heavy quarks [1–5]. Of course, the notion of the intrinsic charm content of the proton was introduced over 30 years ago in Ref. [6]. The study of production mechanisms of heavy quarks provides us with new tests of QCD. In perturbative QCD (pQCD), physical quantities can be expanded into the strong coupling constant $\alpha_s(\mu^2)$. Extensions of the μ scale to large values establish the theoretical analysis that can be described with hard processes. In the case of heavy quark production, the heavy quarks can be produced from the boson–gluon fusion (BGF) according to Fig. 1. That is, in QCD calculations, the production of heavy quarks at HERA proceeds dominantly via the direct BGF where the photon interacts with a gluon from the proton by the exchange of a heavy quark pair.

In this processes all quark flavors lighter than charm are treated as massless, with the massive charm produced dynamically in BGF. Charm production contributes at most 30 % to the total deep inelastic scattering (DIS) cross section at HERA [7]. In the recent measurements of HERA [8], the charm contribution to the structure function at small x is a large fraction of the total. This behavior is directly related to the growth of the gluon density at small x, because gluons couple only through the strong interaction. Consequently, the gluons are not directly probed in DIS, only contributing indirectly via the $g \to q\bar{q}$ transition. This involves the computation of the BGF process $\gamma^\star g \to c\bar{c}$. This process can be created when the squared invariant mass of the hadronic final state is

$$W^2 \geq 4m_c^2.$$

In this paper, we apply the expansion of the gluon distribution at an arbitrary point to the charm structure functions in deep inelastic scattering. Then we

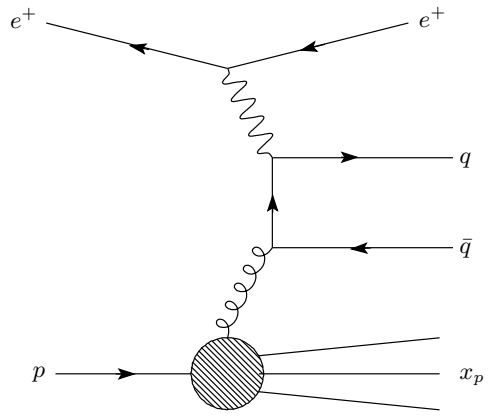

Fig. 1. The photon–gluon fusion

*E-mail: grboroun@gmail.com; boroun@razi.ac.ir
**E-mail: brezaei@razi.ac.ir

present the ratio of the charm structure functions that is independent of the gluon distribution and is useful in extracting the charm structure function from the reduced charm cross section experimental data.

2. CHARM COMPONENTS OF THE STRUCTURE FUNCTIONS

In deep inelastic electron–proton scattering, the heavy-quark contribution to heavy flavor is described by the reaction

$$e(l_1) + P(p) \to e(l_2) + Q(p_1)\overline{Q}(p_2) + X, \qquad (1)$$

where we neglect the contribution of Z-boson exchange and omit charged-current interactions. The deep inelastic electroproduction cross section for the heavy quark–antiquark in the final state can be written as

$$\frac{d^2\sigma^{c\overline{c}}}{dx\,dQ^2} = \frac{2\pi\alpha^2}{xQ^4}(1+(1-y)^2)F_2(x,Q^2,m_c^2) \times \times \left[1 - \frac{y^2}{1+(1-y)^2}R^c\right], \qquad (2)$$

where R^c denotes the ratio of the charm structure functions and the kinematic variables are defined by

$$x = \frac{Q^2}{2p\cdot q}, \quad y = \frac{p\cdot q}{p\cdot l}, \quad Q^2 = -q^2.$$

The deep inelastic charm structure functions ($F_k(x,Q^2,m_c^2)$ for $k = 2, L$) in cross section (2) is given by [9]

$$F_k^c(x,Q^2,m_c^2) = 2xe_c^2\frac{\alpha_s(\mu^2)}{2\pi} \times \times \int\limits_{ax}^{1}\frac{dy}{y}C_{g,k}\left(\frac{x}{y},\zeta\right)g(y,\mu^2), \qquad (3)$$

where

$$a = 1+4\zeta, \quad \zeta \equiv \frac{m_c^2}{Q^2},$$

$g(x,\mu^2)$ is the gluon density, and the mass factorization scale μ, which has been set equal to the renormalization scale, is assumed to be either

$$\mu^2 = 4m_c^2 \quad \text{or} \quad \mu^2 = 4m_c^2 + Q^2.$$

Here, $C_{g,k}^c$ is the charm coefficient function in the LO and NLO analysis:

$$C_{k,g}(z,\zeta) \to C_{k,g}^0(z,\zeta) + + a_s(\mu^2)\left[C_{k,g}^1(z,\zeta) + \overline{C}_{k,g}^1(z,\zeta)\ln\frac{\mu^2}{m_c^2}\right], \qquad (4)$$

where

$$a_s(\mu^2) = \frac{\alpha_s(\mu^2)}{4\pi}$$

and

$$\alpha_s(\mu^2) = \frac{4\pi}{\beta_0\ln(\mu^2/\Lambda^2)} - \frac{4\pi\beta_1}{\beta_0^3}\frac{\ln\ln(\mu^2/\Lambda^2)}{\ln(\mu^2/\Lambda^2)} \qquad (5)$$

in the NLO analysis with

$$\beta_0 = 11 - \frac{2}{3}n_f, \quad \beta_1 = 102 - \frac{38}{3}n_f$$

(n_f is the number of active flavors).

In the LO analysis, the coefficient functions BGF can be found [9] as

$$C_{g,2}^0(z,\zeta) = = \frac{1}{2}\left([z^2+(1-z)^2+4z\zeta(1-3z)-8\zeta^2z^2] \times \times \ln\frac{1+\beta}{1-\beta} + \beta[-1+8z(1-z)-4z\zeta(1-z)]\right), \qquad (6)$$

and

$$C_{g,L}^0(z,\zeta) = -4z^2\zeta\ln\frac{1+\beta}{1-\beta} + 2\beta z(1-z), \qquad (7)$$

where

$$\beta^2 = 1 - \frac{4z\zeta}{1-z}.$$

At the NLO, $O(\alpha_{em}\alpha_s^2)$, the contribution of the photon–gluon component, is usually represented in terms of the coefficient functions $C_{k,g}^1$ and $\overline{C}_{k,g}^1$. The virtual photon–quark(antiquark) fusion subprocesses can be neglected because their contributions to the heavy-quark leptoproduction vanish in the LO and are small in the NLO [1, 10]. In a wide kinematic range, the contributions to the charm structure functions in the NLO are not positive due to mass factorization and are less than 10 %. Therefore, the charm structure functions are dependent on the gluonic observables in the LO and NLO. The NLO coefficient functions are only available as computer codes [9, 10]. But in the high-energy regime ($\zeta \ll 1$), we can use the compact form of these coefficients given in Refs. [11, 12].

3. THE METHOD

We calculate the charm structure functions by using the expansion method for the gluon distribution function. As can be seen, the dominant contribution to the charm structure functions comes from the gluon

density at small x, regardless of the exact shape of the gluon distribution. We substitute

$$y = \frac{x}{1-z}$$

in Eq. (3) to obtain the more useful form

$$F_k^c(x,Q^2,m_c^2) = 2e_c^2\frac{\alpha_s(\mu^2)}{2\pi}\int\limits_{1-\frac{1}{a}}^{1-x} dz C_{g,k}^c(1-z,\zeta)\times \\ \times G\left(\frac{x}{1-z},\mu^2\right), \quad (8)$$

where $G(x) = xg(x)$ is the gluon distribution function. The argument $x/(1-z)$ of the gluon distribution in Eq. (8) can be expanded at an arbitrary point $z = \alpha$ as

$$\left.\frac{x}{1-z}\right|_{z=\alpha} = \frac{x}{1-\alpha}\sum_{k=1}^{\infty}\left[1+\frac{(z-\alpha)^k}{(1-\alpha)^k}\right]. \quad (9)$$

The above series is convergent for $|z-\alpha|<1$. Using this expression, we can rewrite and expand the gluon distribution as

$$G\left(\frac{x}{1-z}\right) = G\left(\frac{x}{1-\alpha}\right) + \\ + \frac{x}{1-\alpha}(z-\alpha)\frac{\partial G\left(\frac{x}{1-a}\right)}{\partial x} + O(z-\alpha)^2. \quad (10)$$

Retaining terms only up to the first derivative in the expansion and integrating, we obtain our master formula

$$F_k^c(x,Q^2,m_c^2) = 2e_c^2\frac{\alpha_s(\mu^2)}{2\pi}A_k(x)\times \\ \times G\left(\frac{x}{1-\alpha}\left(1-\alpha+\frac{B_k(x)}{A_k(x)}\right)\right), \quad (11)$$

where

$$A_k(x) = \int\limits_{1-\frac{1}{\alpha}}^{1-x} C_{g,k}^c(1-z,\zeta)\,dz, \quad (12)$$

and

$$B_k(x) = \int\limits_{1-\frac{1}{\alpha}}^{1-x}(z-\alpha)C_{g,k}^c(1-z,\zeta)\,dz, \quad (13)$$

where $C_{g,k}^c$ is defined in Eq. (4) in the LO and NLO analysis and α has an arbitrary value $0\le\alpha<1$. Equation (10) can be rewritten as

$$F_k^c(x,Q^2,m_c^2) = \\ = 2e_c^2\frac{\alpha_s(\mu^2)}{2\pi}\eta_k G\left(\frac{x}{1-\alpha}(\beta_k-\alpha),\mu^2\right). \quad (14)$$

This result shows that the charm structure functions $F_k^c(x,Q^2)$ at x are calculated using the gluon distribution at

$$\frac{x}{1-\alpha}(\beta_k-\alpha).$$

Therefore, this gluon distribution at $(x/(c-\alpha))(\beta_k-\alpha)$ can be simply extracted from the charm structure functions (F_2^c and F_L^c) at low x according to the coefficients in the limit $x\to 0$ given in Table 1. Moreover, there is a direct relation between the charm structure functions and gluon distribution via the well known Bethe–Heitler process $\gamma^\star g\to c\bar{c}$.

We define the ratio of the charm structure functions and use Eq. (14), so we obtain the equation

$$R^c = \frac{\eta_L}{\eta_2}\frac{G\left(\frac{x}{1-\alpha}(\beta_L-\alpha)\right)}{G\left(\frac{x}{1-\alpha}(\beta_2-\alpha)\right)}. \quad (15)$$

We observe that the right-hand side of this ratio is independent of x and of the gluon distribution input according to the coefficients in Table 1. In the low-x range, we have

$$R^c \approx \frac{\eta_L}{\eta_2}, \quad (16)$$

which is very useful in extracting the charm structure function $F_2^c(x,Q^2)$ from measurements of the doubly differential cross section of inclusive deep inelastic scattering at DESY HERA, independent of the gluon distribution function. Therefore, we can determine the charm structure function in the reduced cross section from the double-differential charm cross section as

$$F_2(x,Q^2,m_c^2) = \frac{\widetilde{\sigma}^{c\overline{c}}(x,Q^2)}{1-\frac{y^2}{1+(1-y)^2}R^c}, \quad (17)$$

where R^c is defined in Eq. (16) and Table 1 and $\widetilde{\sigma}^{c\overline{c}}$ is taken from Ref. [13]. The error bars in our determination can be described by the expression (Table 1)

$$\delta_{F_2^{c\overline{c}}} = F_2^{c\overline{c}}\left[\frac{\delta_{\widetilde{\sigma}^{c\overline{c}}}}{\widetilde{\sigma}^{c\overline{c}}} + \frac{\frac{y^2}{1+(1-y)^2}\delta_{R^c}}{1-\frac{y^2}{1+(1-y)^2}R^c}\right]. \quad (18)$$

4. RESULTS AND DISCUSSION

For the calculation of the charm structure functions ($F_2^{c\overline{c}}$ and $F_L^{c\overline{c}}$), we choose $\Lambda = 0.224$ GeV and $m_c = 1.5$ GeV; we recall that the dominant uncertainty in QCD calculations arises from the uncertainty in the

Table 1. The constant values in this analysis at Q^2 values in the limit $x \to 0$

Q^2, GeV^2	η_2	δ_{η_2}	β_2	δ_{β_2}	η_L	δ_{η_L}	β_L	δ_{β_L}	R^c	δ_{R^c}
8.5	0.4645	$1.95 \cdot 10^{-3}$	1.8393	$2 \cdot 10^{-4}$	0.0504	$4 \cdot 10^{-4}$	1.7853	$1 \cdot 10^{-4}$	0.1085	$4.5 \cdot 10^{-4}$
12	0.5763	$3.7 \cdot 10^{-3}$	1.8083	$3.5 \cdot 10^{-4}$	0.0730	$9 \cdot 10^{-4}$	1.7453	$1.5 \cdot 10^{-4}$	0.1267	$8 \cdot 10^{-4}$
15	0.6546	$5.45 \cdot 10^{-3}$	1.7883	$5 \cdot 10^{-4}$	0.0901	$1.45 \cdot 10^{-3}$	1.7200	$1 \cdot 10^{-4}$	0.1377	$1.1 \cdot 10^{-3}$
20	0.7611	$8.45 \cdot 10^{-3}$	1.7632	$7 \cdot 10^{-4}$	0.1145	$2.45 \cdot 10^{-3}$	1.6883	$2 \cdot 10^{-4}$	0.1505	$1.6 \cdot 10^{-3}$
25	0.8469	0.0114	1.7447	$1 \cdot 10^{-3}$	0.1347	$3.6 \cdot 10^{-3}$	1.6654	$2.5 \cdot 10^{-4}$	0.1590	$2.1 \cdot 10^{-3}$
35	0.9795	0.0173	1.7190	$1.35 \cdot 10^{-3}$	0.1659	$5.8 \cdot 10^{-3}$	1.6343	$3 \cdot 10^{-4}$	0.1693	$2.9 \cdot 10^{-3}$
45	1.0800	0.0227	1.7016	$1.65 \cdot 10^{-3}$	0.189	$7.9 \cdot 10^{-3}$	1.6139	$3.5 \cdot 10^{-4}$	0.1749	$3.6 \cdot 10^{-3}$
60	1.1953	0.0300	1.6838	$2.05 \cdot 10^{-3}$	0.2144	0.0107	1.5936	$3.5 \cdot 10^{-4}$	0.1793	$4.45 \cdot 10^{-3}$
120	1.4709	0.052	1.6500	$3.1 \cdot 10^{-3}$	0.2681	0.019	1.5568	$3.5 \cdot 10^{-4}$	0.1820	$6.5 \cdot 10^{-3}$
200	1.6698	0.0718	1.6307	$3.85 \cdot 10^{-3}$	0.2996	0.026	1.5387	$3 \cdot 10^{-4}$	0.1791	$7.85 \cdot 10^{-3}$
300	1.8252	0.089	1.6187	$4.3 \cdot 10^{-3}$	0.3198	0.0316	1.5283	$2 \cdot 10^{-4}$	0.1748	$8.8 \cdot 10^{-3}$

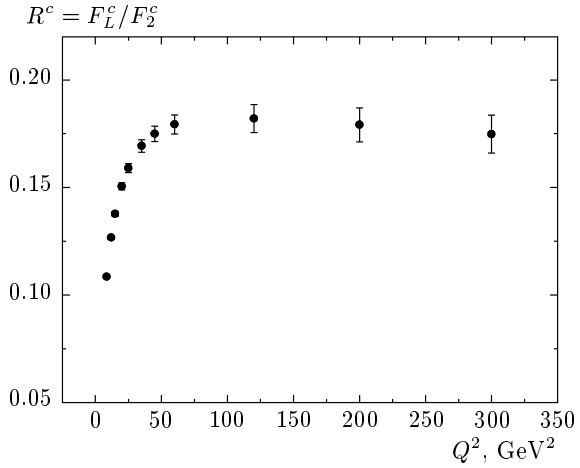

Fig. 2. The ratio R^c evaluated as a function of Q^2 in the NLO analysis from Eq. (16). The error bars are the theoretical uncertainty using the renormalization scales $\mu^2 = 4m_c^2$ and $\mu^2 = 4m_c^2 + Q^2$

charm quark mass. Since the contribution of the longitudinal charm structure function to the DIS charm cross section (i. e., Eq. (2)) is proportional to y^2, it follows that the $F_2^{c\overline{c}}$ term dominates at $y \leq 0.08$ and the relation $\widetilde{\sigma}^{c\overline{c}} = F_2^{c\overline{c}}$ holds to a very good approximation. Hence, the contribution of the second term in the right-hand Eq. (2) can be significant only at $y > 0.08$. Therefore, for $y > 0.08$, the ratio of the charm structure functions is very useful. We see from Fig. 2 that this ratio agrees with the results Refs. [4] and [11] at low x. In the NLO analysis, it decreases as Q^2 increases, and this is familiar from the Callan–Gross ratio. As we can see in this figure, this ratio has a value $0.1 < R^c < 0.2$ in a wide region of Q^2.

We now extract $F_2^{c\overline{c}}$ from the H1 measurements of the reduced charm cross section [13] in Eq. (17) with respect to Eq. (16) for $Q^2 \geq 8.5$ GeV^2. Our NLO results for the charm structure function are presented in Table 2, where they are compared with the experimental values from H1 data; they are compatible with the HVQDIS and CASCADE programs [14, 15] as we can see from Table 11 in Ref. [13] (arXiv:1106.1028v1). The error bars in Table 2 are according to the theoretical uncertainty related to the freedom in the choice of the renormalization scales in the ratio of the charm structure function and the experimental total errors related to the results in Ref. [13] according to Eq. (18). A comparison between our obtained values for the charm structure function and the existing data indicate that the ratio R^c can be determined with reasonable precision at any y value.

To test the validity and correctness of our obtained charm structure functions with respect to the gluon distribution function in Eq. (14), we obtained the charm structure functions from the gluon distribution input, which is usually taken from NLOGRV [9] or Block [16] parameterizations. The gluon distribution input is dependent on the point of expansion α. To estimate the theoretical uncertainty resulting from this, we choose $\alpha = 0$ and $\alpha = 0.8$ in the renormalization scale

$$\mu^2 = 4mc^2 + Q^2.$$

In Figs. 3–6, we observe that the theoretical uncertainty related to the freedom in the choice of α is very small at the renormalization scales. As can be seen from Figs. 3 and 4, the better choice for the expansion point

Table 2. The charm structure function determined based on the reduced charm cross section data accompanied with errors

Q^2, GeV^2	x	y	$\widetilde{\sigma}^{c\overline{c}}$	$\delta_{\widetilde{\sigma}^{c\overline{c}}}$, %	$F_2^{c\overline{c}}$ (Ref. [13])	$\delta_{F_2^{c\overline{c}}}$, %	$F_2^{c\overline{c}}$ (Our Results)	$\delta_{F_2^{c\overline{c}}}$
8.5	0.00050	0.167	0.176	14.8	0.176	1.0	0.1763	14.8
8.5	0.00032	0.262	0.186	15.5	0.187	1.0	0.1869	15.6
12	0.00130	0.091	0.150	18.7	0.150	1.0	0.1501	18.7
12	0.00080	0.148	0.177	15.9	0.177	1.1	0.1773	15.9
12	0.00050	0.236	0.240	11.2	0.242	1.0	0.2441	11.4
12	0.00032	0.369	0.273	13.8	0.277	1.1	0.2764	14.0
20	0.00200	0.098	0.187	12.7	0.188	1.1	0.1871	12.7
20	0.00130	0.151	0.219	11.9	0.219	1.1	0.2194	11.9
20	0.00080	0.246	0.274	10.2	0.276	1.0	0.2756	10.3
20	0.00050	0.394	0.281	13.8	0.287	1.1	0.2859	14.0
35	0.00320	0.108	0.200	12.7	0.200	1.1	0.2002	12.7
35	0.00200	0.172	0.220	11.8	0.220	1.0	0.2206	11.8
35	0.00130	0.265	0.295	9.70	0.297	1.0	0.2973	9.8
35	0.00080	0.431	0.349	12.7	0.360	1.1	0.3575	13.0
60	0.00500	0.118	0.198	10.8	0.199	1.1	0.1983	10.8
60	0.00320	0.185	0.263	8.40	0.264	1.0	0.2640	8.5
60	0.00200	0.295	0.335	8.80	0.339	1.0	0.3385	8.9
60	0.00130	0.454	0.296	15.1	0.307	1.0	0.3047	15.6
120	0.01300	0.091	0.133	14.1	0.133	1.2	0.1331	14.1
120	0.00500	0.236	0.218	11.1	0.220	1.1	0.2194	11.2
120	0.00200	0.591	0.351	12.8	0.375	2.9	0.3712	13.6
200	0.01300	0.151	0.161	11.9	0.160	2.7	0.1604	11.9
200	0.00500	0.394	0.237	13.5	0.243	2.9	0.2419	13.8
300	0.02000	0.148	0.117	18.5	0.117	2.9	0.1173	18.5
300	0.00800	0.369	0.273	12.7	0.278	2.9	0.2777	12.9

for the charm structure function F_2^c is $\alpha \approx 0.5$ because this point is favored by the current data. This means that in this kinematic region, the longitudinal momentum of the gluon x_g is more than three times the value of the longitudinal momentum of the probed charm quark–antiquark in the BGF process. We compared our results for the charm structure function to the DL model [17–19], H1 data [13], and the color dipole model [20]. In Figs. 5 and 6, the better choice of the expansion point for the longitudinal charm structure function F_L^c is $\alpha \geq 0.8$, as compared only to the color dipole model [20]. As can be seen from these figures, the increase in the charm structure functions $F_k^c(x, Q^2)$ toward low x is consistent and compatible with the experimental data and theoretical models.

5. CONCLUSION

In summary, we have used the expansion method for the low-x gluon distribution and derived a compact formula for the ratio $R^c = F_L^{c\overline{c}}/F_2^{c\overline{c}}$ of the charm structure functions in the NLO analysis. We observed that this ratio is independent of x and of the parton distribution function input, and is also useful in extracting the charm structure function from the reduced charm cross section. Based on the reduced charm cross section in the low-x region, an approximate method for the calculation of the charm structure function $F_2^{c\overline{c}}$ is presented. Careful investigation of our results shows a good agreement with the recent published charm structure functions $F_2^{c\overline{c}}$ and other theoretical models within

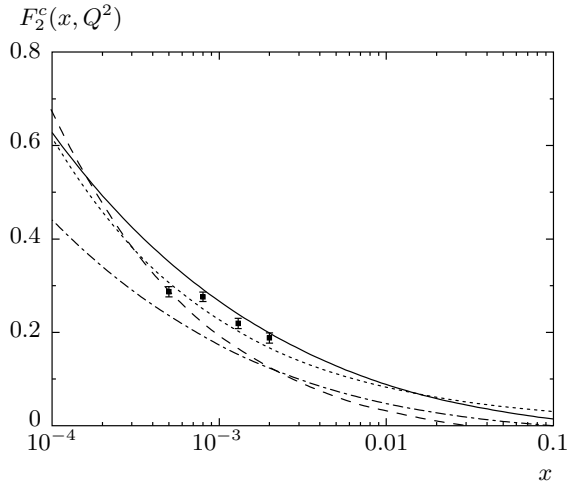

Fig. 3. The charm structure function ($F_2^{c\overline{c}}$) obtained at $Q^2 = 20$ GeV^2 with respect to the input gluon distribution NLO–GRV parameterization [9]. The solid line corresponds to the expansion point $\alpha = 0$ and the dash-dotted line corresponds to the expansion point $\alpha = 0.8$. These are compared with the DL fit [17–19] (dotted line), the color dipole model [20] (dashed line), and H1 data [13] (squares) accompanied with total errors at the renormalization scale $\mu^2 = 4m_c^2 + Q^2$

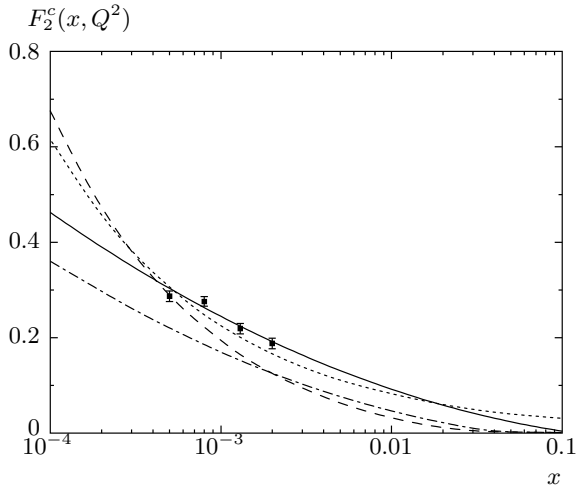

Fig. 4. The charm structure function ($F_2^{c\overline{c}}$) obtained at $Q^2 = 20$ GeV^2 with respect to the input gluon distribution Block fit [16]. The solid line corresponds to the expansion point $\alpha = 0$ and the dash-dotted line corresponds to the expansion point $\alpha = 0.8$. These are compared with the DL fit [17–19] (dotted line), the color dipole model [20] (dashed line), and H1 data [13] (squares) accompanied with total errors at the renormalization scale $\mu^2 = 4m_c^2 + Q^2$

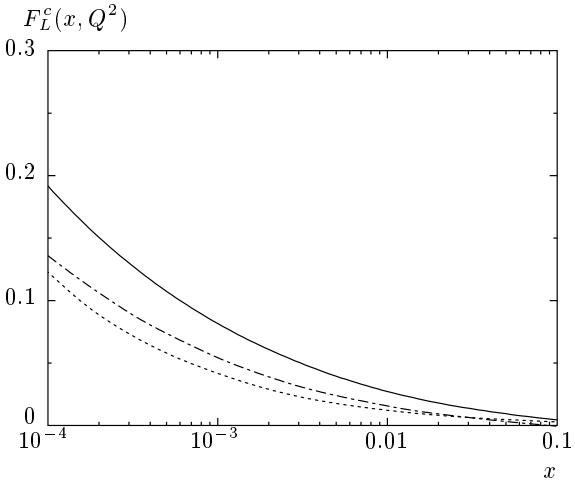

Fig. 5. The longitudinal charm structure function ($F_L^{c\overline{c}}$) obtained at $Q^2 = 20$ GeV^2 with respect to the input gluon distribution NLO–GRV parameterization [9]. The solid line corresponds to the expansion point $\alpha = 0$ and the dash-dotted line corresponds to the expansion point $\alpha = 0.8$. These are compared with the color dipole model [20] (dashed line) at the renormalization scale $\mu^2 = 4m_c^2 + Q^2$

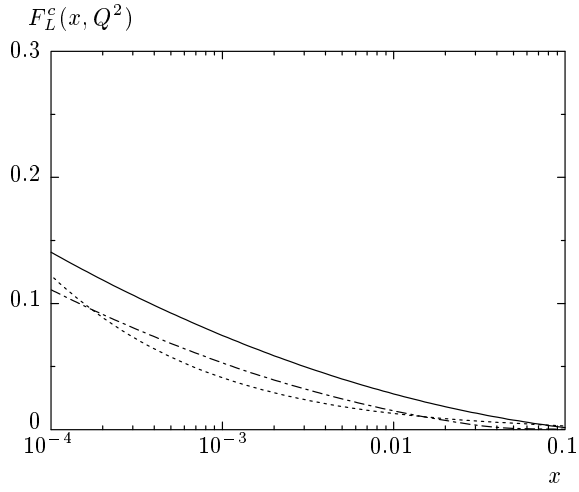

Fig. 6. The longitudinal charm structure function ($F_L^{c\overline{c}}$) obtained at $Q^2 = 20$ GeV^2 with respect to the input gluon distribution Block fit [16]. The solid line corresponds to the expansion point $\alpha = 0$ and the dash-dotted line corresponds to the expanding point $\alpha = 0.8$. These are compared with the color dipole model [20] (dashed line) at the renormalization scale $\mu^2 = 4m_c^2 + Q^2$

errors due to the expansion point and the renormalization scales.

REFERENCES

1. A. Vogt, arXiv:hep-ph:9601352v2.
2. H. L. Lai and W. K. Tung, Z. Phys. C **74**, 463 (1997).
3. A. Donnachie and P. V. Landshoff, Phys. Lett. B **470**, 243 (1999).
4. N. Ya. Ivanov, Nucl. Phys. B **814**, 142 (2009); N. Ya. Ivanov and B. A. Kniehl, Eur. Phys. J. C **59**, 647 (2009).
5. F. Carvalho et al., Phys. Rev. C **79**, 035211 (2009).
6. S. J. Brodsky, P. Hoyer, C. Peterson, and N. Sakai, Phys. Lett. B **93**, 451 (1980); S. J. Brodsky, C. Peterson, and N. Sakai, Phys. Rev. D **23**, 2745 (1981).
7. K. Lipta, PoS (EPS-HEP)313, (2009).
8. C. Adloff et al. [H1 Collaboration], Z. Phys. C **72**, 593 (1996); J. Breitweg et al. [ZEUS Collaboration], Phys. Lett. B **407**, 402 (1997); C. Adloff et al. [H1 Collaboration], Phys. Lett. B **528**, 199 (2002); S. Aid et al. [H1 Collaboration], Z. Phys. C **72**, 539 (1996); J. Breitweg et al. [ZEUS Collaboration], Eur. Phys. J. C **12**, 35 (2000); S. Chekanov et al. [ZEUS Collaboration], Phys. Rev. D **69**, 012004 (2004); Aktas et al. [H1 Collaboration], Eur. Phys. J. C **45**, 23 (2006); F. D. Aaron et al. [H1 Collaboration], Eur. Phys. J. C **65**, 89 (2010).
9. M. Gluk, E. Reya, and A. Vogt, Z. Phys. C **67**, 433 (1995); Eur. Phys. J. C **5**, 461(1998).
10. E. Laenen, S. Riemersma, J. Smith, and W. L. van Neerven, Nucl. Phys. B **392**, 162 (1993).
11. A. Y. Illarionov, B. A. Kniehl, and A. V. Kotikov, Phys. Lett. B **663**, 66 (2008).
12. S. Catani, M. Ciafaloni, and F. Hautmann, Preprint CERN-Th.6398/92; in *Proc. of the Workshop on Physics at HERA*, Hamburg (1991), Vol. 2, p. 690; S. Catani and F. Hautmann, Nucl. Phys. B **427**, 475 (1994); S. Riemersma, J. Smith, and W. L. van Neerven, Phys. Lett. B **347**, 143 (1995).
13. F. D. Aaron et al. [H1 Collaboration], Phys. Lett. B **665**, 139 (2008); Eur. Phys. J. C **71**, 1509 (2011); Eur. Phys. J. C **71**, 1579 (2011); arXiv:1106.1028v1; arXiv:0911.3989v1.
14. H. Jung, CASCADE V2.0, Comp. Phys. Commun. **143**, 100 (2002).
15. B. W. Harris and J. Smith, Nucl. Phys. B **452**, 109 (1995); Phys. Rev. D **57**, 2806(1998).
16. M. M. Block, L. Durand, and D. W. Mckay, Phys. Rev. D **77**, 094003 (2008).
17. A. Donnachie and P. V. Landshoff, Z. Phys. C **61**, 139 (1994); Phys. Lett. B **518**, 63 (2001); Phys. Lett. B **533**, 277 (2002); Phys. Lett. B **470**, 243 (1999); Phys. Lett. B **550**, 160 (2002).
18. R. D. Ball and P. V. Landshoff, J. Phys. G **26**, 672 (2000).
19. P. V. Landshoff, arXiv:hep-ph/0203084.
20. N. N. Nikolaev and V. R. Zoller, Phys. Lett. B **509**, 283 (2001).